# Analysis of a Unidirectional Power Electronic Transformer for Distribution Network

**Ereola Aladesanmi[*], Priye Kenneth Ainah[**]**

[*] Department of Electrical, Electronic and Computer Engineering,
University of KwaZulu-Natal, Durban, South Africa
[**] Department of Electrical and Electronic Engineering,
Niger Delta University, Amassoma, Wilberforce Island, Bayelsa State

DOI: 10.29322/IJSRP.12.06.2022.p12628
http://dx.doi.org/10.29322/IJSRP.12.06.2022.p12628

Paper Received Date: 20th May 2022
Paper Acceptance Date: 5th June 2022
Paper Publication Date: 14th June 2022

***Abstract***- This paper presents a unidirectional three-stage power electronic transformer (PET) for interfacing the low voltage (LV) and medium voltage (MV) distribution networks. The input stage of the PET system converts the incoming medium voltage to DC voltage. The second stage is the isolation stage which consist of a converter and rectifier that are connected to the primary and secondary side of the transformer respectively while the output stage is made up of a 2-level 3-phase inverter which connects the LV distribution network.
A 500 KVA, 11 / 0.415 kV PET system is simulated with a 38-bus distribution network in Simulink and the performance of the PET device was evaluated under fault, load variation and unbalance voltage conditions. The simulation results show the potency of the PET device for power quality improvement in distribution network.

***Index Terms***- Unidirectional power electronic transformer, Power quality, Distribution network, Power Electronic Converter

## I. INTRODUCTION

In recent years, the liberalization of energy markets, rising energy demand, and environmental concerns have increased the integration of photovoltaic (PV) system into the distribution network [1]–[5]. Dual power flow, sufficient energy storage capacity, and advanced grid integration technologies are some of the potentials of PV system for future smart grid architecture [6]. However, power quality problems may arise due to the high penetration of PV system into the distribution systems [7]–[12]. Furthermore, sudden connection and disconnection of RES may become a challenge to the distribution networks. Power electronic transformer (PET) has been identified as an emerging technology to overcome these challenges and also, to achieve the benefits associated with the integration of renewable energy technologies in the future smart grid [13]–[21]. PET is a power conversion device that performs voltage transformation using power electronic converters installed on both side of the transformer.
PET enhances the reliability and efficiency of power system networks through quick response to power quality issues, fault isolation, and integration of renewable energy technologies [22]–[26]. A 15 kV 1.2 MVA single phase used for railway systems, and 300 kVA UNIFLEX for power management are some of the prototypes designed by researchers [45-48]. Other works done by researchers are presented in [19], [27]–[37]. PET application includes; generation source and distribution grid interface, interconnecting two distribution grid, and connection between distribution network and loads. However, this paper introduces three-stage PET for interfacing MV and LV grid with loads.
The aim of the paper is: to design and simulate a three-phase 11-kV/415-V 500-kVA unidirectional PET device for +interfacing the MV and LV distribution network using Simulink, and to evaluation it's performance in the distribution network under fault and various power quality issues.

## II. MATERIALS AND METHOD

### A. *Materials used for the Analysis*

The distribution system used for the analysis comprises of 38 buses, 37 branches and 36 loads distributed across the network as shown in Fig 1. The network comprises of four zones. Zone A is the MV distribution section which is made up of 11kV buses while zone B, C, and D are LV distribution lines connecting the MV distribution section via the 11/0.415kV, 500kVA PET, and the one-line diagram as shown in Fig 1. All lines in the distribution network have the same values of resistance (R = 0.01273 Ω) and reactance (L= 0.9337 mH). The distribution network and power electronic transformers (PETs) are model in Simulink. The parameters of the power electronic transformer used in the simulation are listed in Table 1 while the load parameters are given in the Appendix

Table 1: Power electronic transformer parameters

| Three Stage Power Converters Parameters | Values |
|---|---|
| Transformer rate power | 500 kVA |
| Grid voltage | 11 kV |
| Capacitance ($C_{dc1}$) (DC-link) | 1500000 mF |
| Capacitance ($C_{dc2}$) (DC-link) | 1500000 mF |
| Grid frequency | 50 Hz |
| Filter resistance (Primary side) | 5 Ω |
| Filter inductance (Primary side) | 624 mH |
| Filter capacitance (Primary side) | 20 µF |
| Capacitance ($C_{dc3}$) (DC-link) | 7500 µF |
| Capacitance ($C_{dc4}$) (DC-link) | 7500 µF |
| Arm resistance | 0.5 Ω |
| Arm inductance | 550 mH |
| Damping resistance (Secondary side) | 0.2 Ω |
| Filter inductance (Secondary side) | 1 mH |
| Filter capacitance (Secondary side) | 470 µf |
| Transformer operation frequency | 2 kHz |

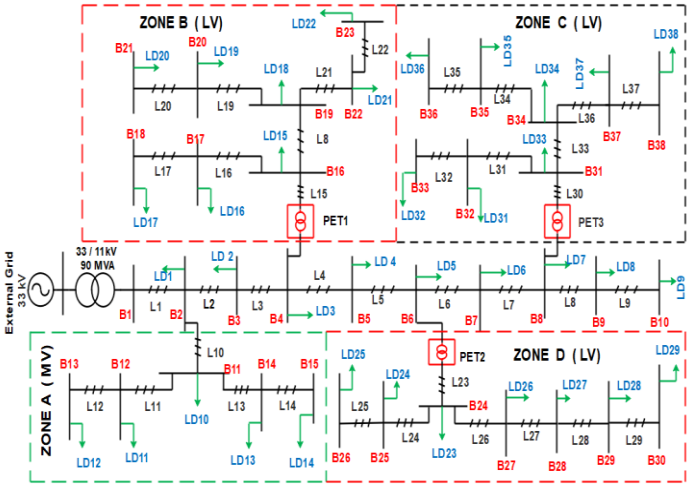


Fig. 1 One-line Network diagram under investigation

**B. *Methodology***

The three-phases 11 / 0.415 kV, 500 kVA unidirectional PET consist of three stages. The input, output and the isolation stages are shown in Fig 2. PET is made up of 3-phase, 3-level rectifier which converts the AC voltage to DC voltage and back to AC voltage. The input part of the isolation stage consists of a 3-phase inverter (DC-AC) which is connected to the primary side of the transformer while the secondary side is connected to a 3-phase rectifier (AC-DC). The input part of the isolation stage converts the DC voltage into a high-frequency PWM signal which is then converted to DC voltage by the rectifier. The 3 -levels converter at the input and middle stage reduces the semiconductor device stress ratio and enhance the performance of the distribution network. The output stage consists of a 2-level 3-phase inverter that connects the LV side. The use of a 2-level inverter is due to the fact that it is cheaper, simple and can be connected directly to a 0.415 kV distribution feeder and load. The three stages of the PET structure and the control schemes are discussed in the subsection below.

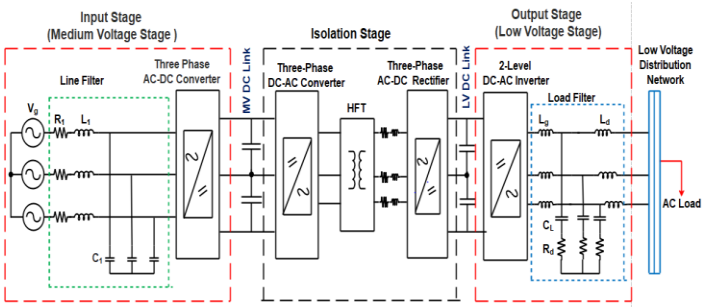


Fig .2. Schematic configuration of three-stage power electronic transformer

B.1 *PET Input Stage Mathematical Model*

The input stage is made up of a 3-level, 3-phase rectifier which convert the incoming medium voltage to DC voltage. The input stage is connected to a MV distribution network via a damped LC filter. The MV side dc-link closed-loop control system allows the reactive power adjustment and stabilized the LV side dc-link voltage. The rectifier control determines the input current, power factor, and maintain a constant DC-link reference voltage. A rotating d-q reference frame is used to develop the control system [38]–[41]. The three phases PWM converter with the control configuration is shown in Fig 3.

Equation 1 and 2 represent the input stage mathematical model in the d-q reference frame.

$$L_{E1}\frac{\partial i_{E1d}}{\partial t} = \omega L_{E1} i_{E1q} + V_{1d} - V_{E1d} \qquad (1)$$

$$L_{E1}\frac{\partial i_{E1q}}{\partial t} = \omega L_{E1} i_{E1d} + V_{1q} - V_{E1q} \qquad (2)$$

where $L_{E1}$ is the interface inductances, $i_{E1}$ is the line current $[i_{Ea}, i_{E1b}, i_{E1c}]$ is the primary side line current vectors, $V_{E1} = [V_{E1a}, V_{E1b}, V_{E1c}]$ is the primary side voltage vectors, $V_1 = [V_{1a}, V_{1b}, V_{1c}]$ is the grid side input voltage, and $\omega$ is the angular frequency.

Equation 3 and 4 represent the close loop control model and the rectifier output voltage in the d-q reference frame.

$$V_d^* = -\left(K_{ip} + \frac{K_{i1}}{s}\right)(i_d^* - i_{sd}) + \omega L_{isq} + V_{sd} \qquad (3)$$

$$V_q^* = -\left(K_{ip} + \frac{K_{i1}}{s}\right)(i_q^* - i_{sq}) - \omega L_{isd} + V_{sq} \qquad (4)$$

where $K_{ip}$ and $K_{i1}$ are the control coefficient. The output voltage of the rectifier is compared with the reference voltage and the error is used to generate $i_d^*$ through the proportional-integral (PI) controller while $i_q^*$ which is the reactive current reference is set at

zero, causing the grid side to have a unity power factor. The input currents are transformed into the dq reference component ($i_d$ and $i_q$ ) in the inner current loop and it is compared with $i_d^*$ and $i_q^*$ and the error is formulated to wave signal by the PI controller [42].

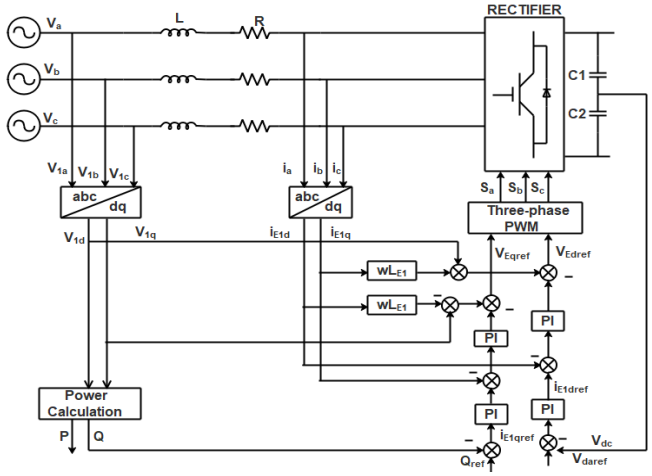


Fig. 3. Input stage configuration with the control scheme

## B.2. *PET Isolated Stage*

The isolation stage consists of three major parts; dc-ac converter which is directly connected to the primary side of the high frequency transformer (HFT). The second part is the HFT connected in delta-delta configuration. Aside from the size reduction, HFT provides electric isolation between the MV and LV sides of the transformer. The third part is the AC-DC converter which converts the AC voltage from the secondary side of HFT to dc voltage and provides the required DC link voltage for the output stage of the transformer. The active power flow depends on the phase shift ratio between the primary and the secondary voltage of the HFT. Fig 4 shows the isolation stage configuration and control scheme. The outer loop regulates the capacitor voltage $V_{dc2}$ and the inner loop regulates the transformer inductance current $i_{dc2}$ .The control response of the system is accelerated by the combination of the two loops. The average power flow through the transformer is given as:

$$P_{AV} = \frac{\left({}^{V_{dc1}}/_{M}\right)\cdot V_{dc2}}{\omega \cdot L} \cdot \varphi \cdot \left(1 - \frac{|\varphi|}{\pi}\right) \qquad (5)$$

where;

M is the transformer ratio, ω is the angular frequency, L is the transformer secondary side leakage inductance, $V_{dc1}$ and $V_{dc2}$ are capacitor DC voltages., and φ is the phase shift angle,

## III. RESULTS AND ANALYSIS

This section shows the impact of the PET device under line to ground fault (LG), load variation and an unbalance voltage situation.

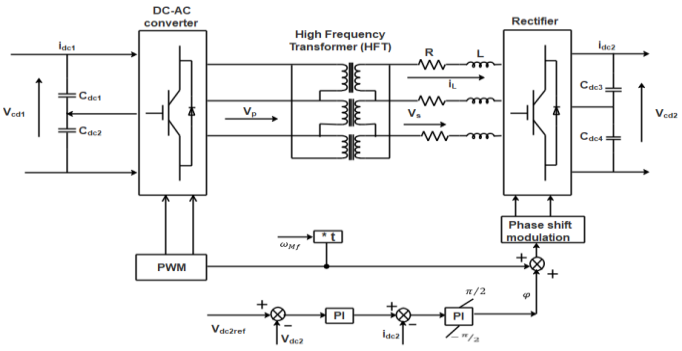


Fig 4. Isolation stage configuration and control

## B.3. *PET Output Stage*

The output stage comprises of 2-level 3-phase PWM inverter that converts the DC voltage from the isolation stage to AC voltage which is then connected to the LV distribution network via a damped LCL filter. The output stage maintain a constant voltage amplitude during grid perturbation. Fig.5 shows the output structure and control principle.

The equations for the output stage model are given in Eq.6 and Eq.7.

$$L_{E2}\frac{\partial i_{E2d}}{\partial t} = \omega L_{E2} i_{e2q} + V_{2d} - V_{E2d} \qquad (6)$$

$$L_{E2}\frac{\partial i_{E2q}}{\partial t} = -\omega L_{E2} i_{E2d} + V_{2d} - V_{E2q} \qquad (7)$$

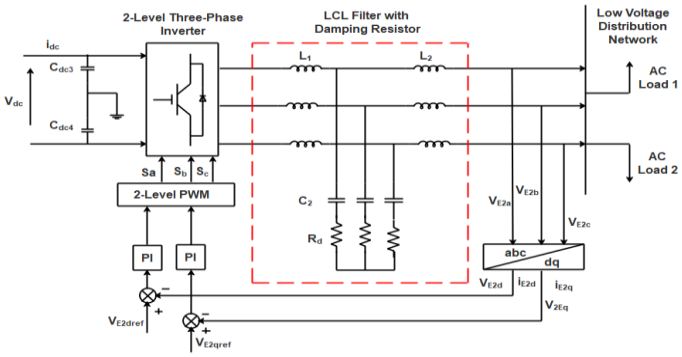


Figure 5. Output structure and control

### A. *Performance of PET under Line to Ground (LG) fault*

It is assumed that the LG fault occurs in zone A (MV) and at line 11 causing voltage swell on the grid. Fig. 6 and 7 show the transformer response to the fault effect on the grid. As depicted in

Fig. 6 (a,b), the situation only affects the medium voltage zone, and bus 4 and bus 8 that connect zone B and C directly to the medium voltage see Fig 6(b) and Fig 7(a). The situation did not propagate to the secondary side (output) of PET as can be seen in figure 6(c). Also, the fault did not escalate to other zones on the grid, as can be seen in Fig. 7 (b,c).

Also, it was assumed that the fault occurs at Low voltage distribution network line 32 see zone C Fig. 6. Figs 9 and 10 show the response of the transformer to the situation on the grid.

As shown in Fig. 8 (b and c), only secondary parts (output) of PET 3 in zone C were affected, and the primary side (Input) of the transformer was not affected Fig.8 (a). Fig.9 (a-c) shows that the situation did not propagate to other zones on the grid. The analysis in Figs. 8 and 9 display the capability of the transformer in isolating the input side from the output via the isolation stage and thus preventing the propagation of fault across the grid. It is assumed that Line to line fault occurred at line 29, on the low voltage side (secondary side) of PET 2 in zone D between 0.15 and 0.25s causing voltage sag. Fig. 10 and 11 show the transformer's response to the situation. As depicted in Fig.10 the distorted voltages and currents at the low voltage (output) side of the transformer did not affect the medium (input) side voltage and current. Fig.11 (a, b) shows that the situation did not propagate to other zones of the grid which also prove the efficacy of the transformer in preventing the situation across the grid.

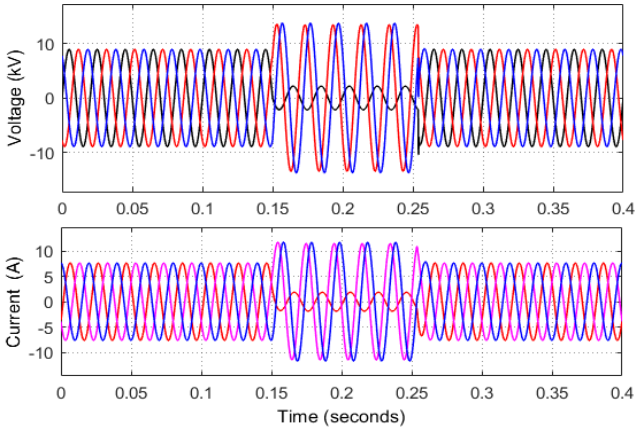


(a)

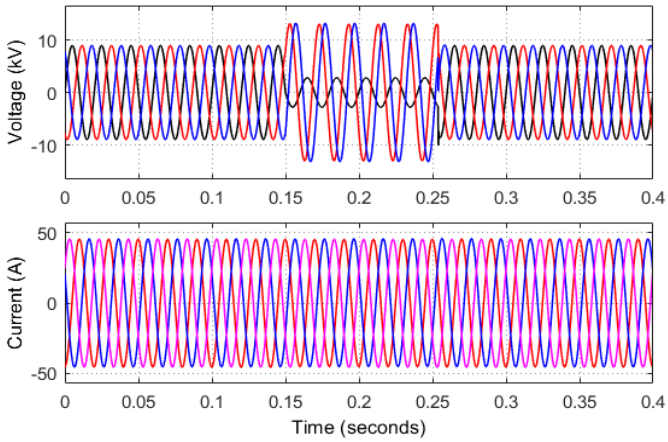


(b)

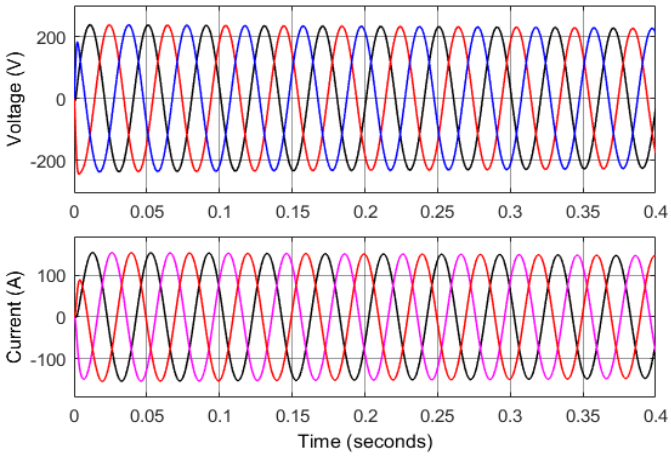


(c)

Fig. 6. Fault at line 11. **(**a) Voltage and current at bus14, (b**)** PET 1 input voltage and current, **(**c**)** PET 1 output voltage and current

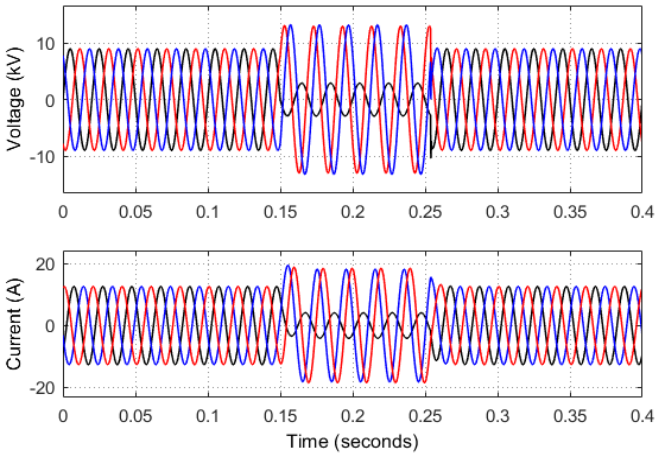


(a)

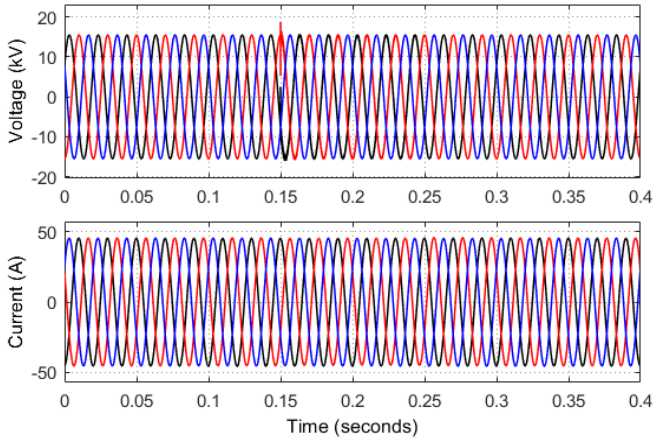


(b)

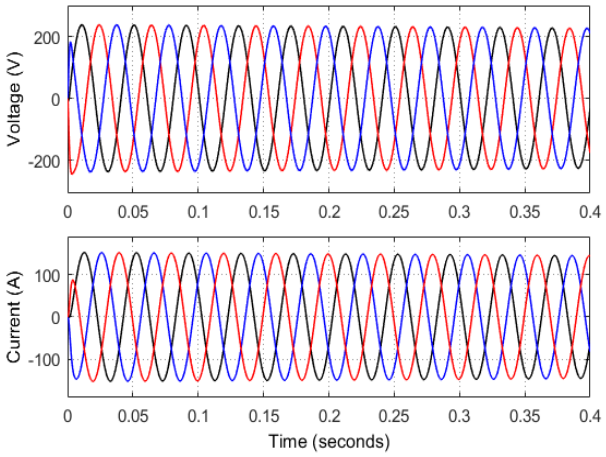


(c)

Fig.7 Fault at line 11. (a) Voltage and current at Bus 8 PET 3 PCC, (b) PET 3 Output voltage and current, (c) PET 3 Input voltage and current

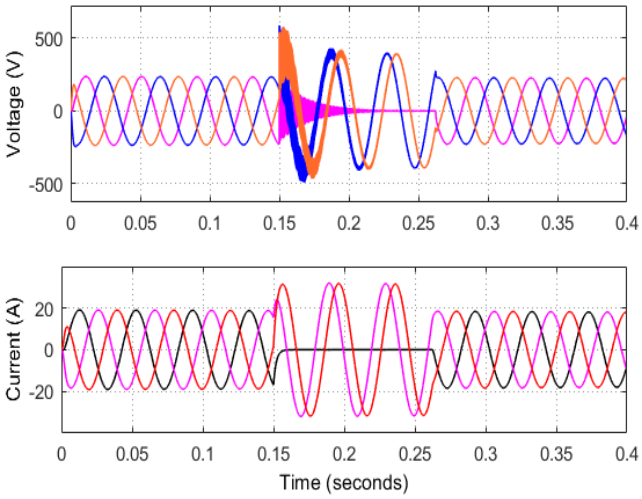


(c)

Fig. 8. Fault at line 32. (a) PET 3 Input voltage and current, (b) PET 3 output voltage and current (c) PET3 Load voltage and current.

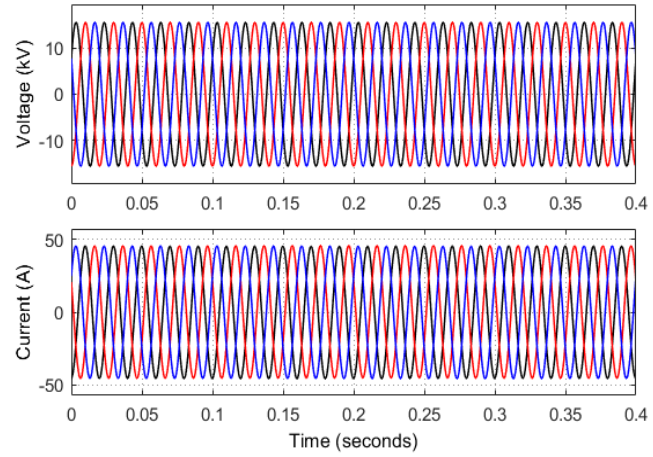


(a)

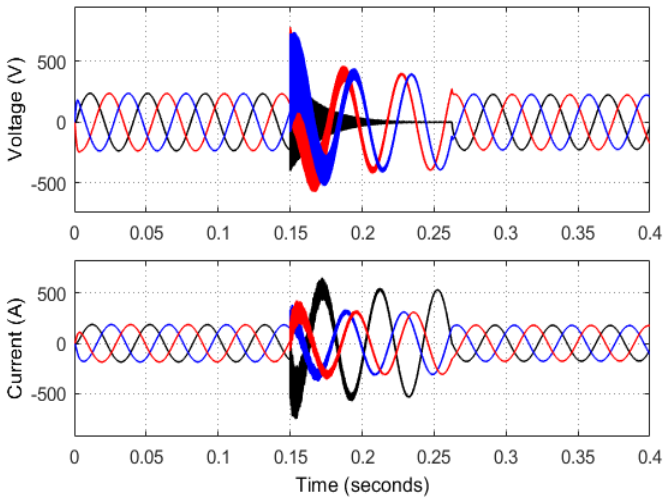


(b)

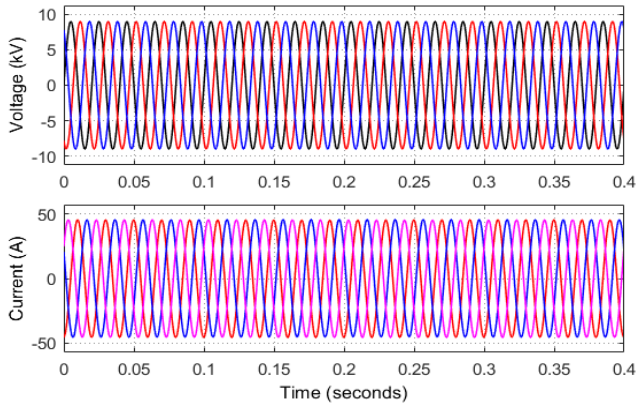


(a)

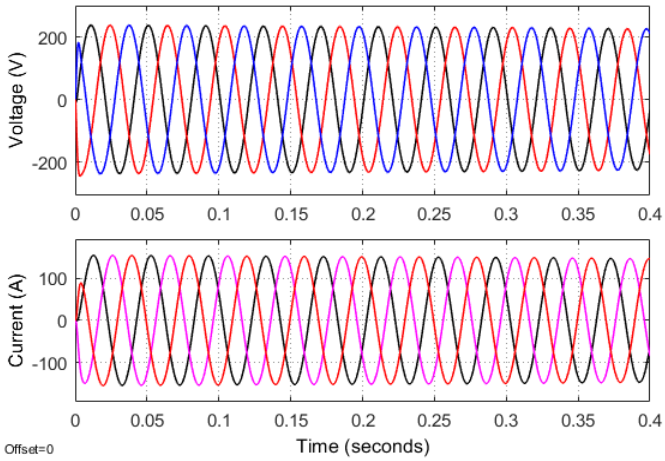


(b)

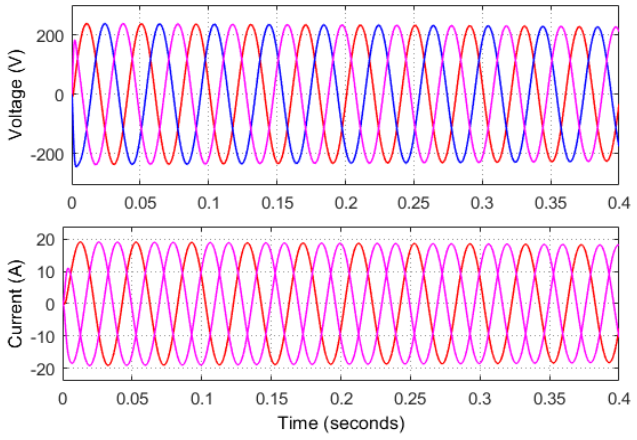


(c)

Fig.9. Fault at line 32. (a**)** PET 1 Input voltage and current, **(**b**)** PET 1 output voltage and current (c**)** PET1 Load voltage and current**.**

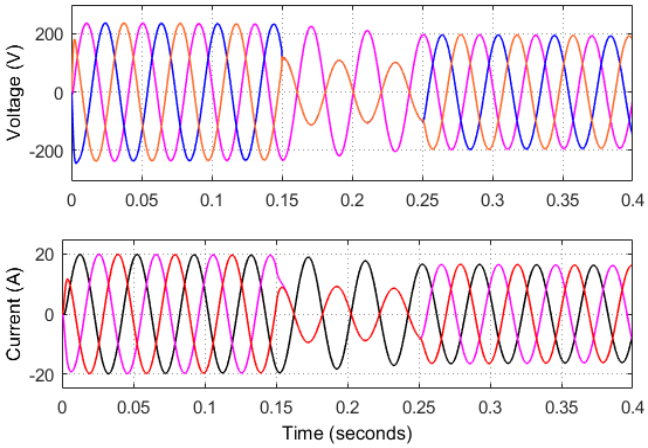


(c)

Fig. 10. Fault at line 32. (a **)** PET 2 Input voltage and current, **(**b**)** PET 2 Output voltage and current (c**)** PET2 Load voltage and current**.**

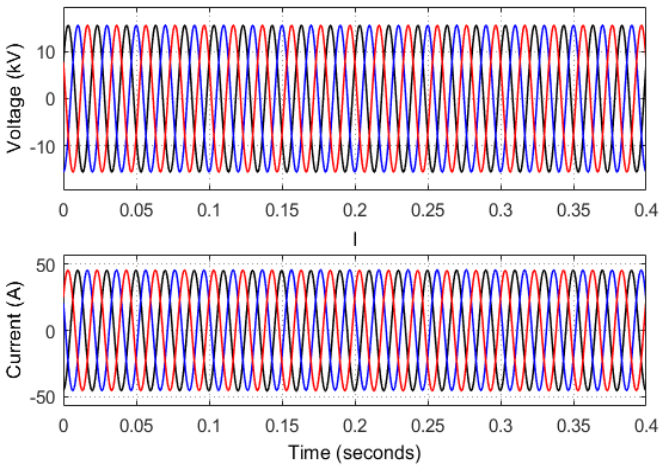


(a)

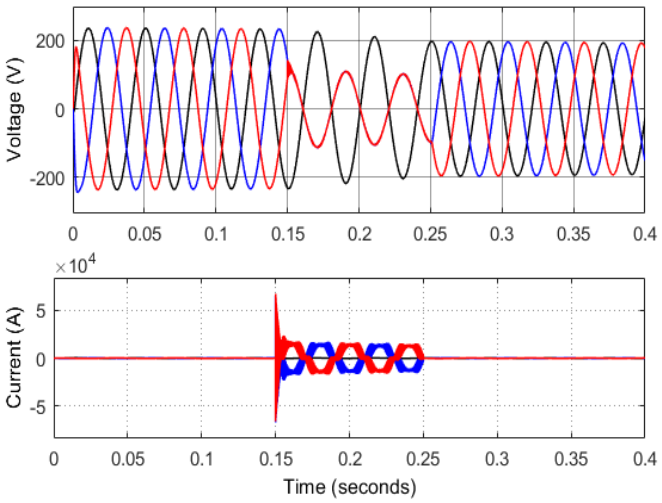


(b)

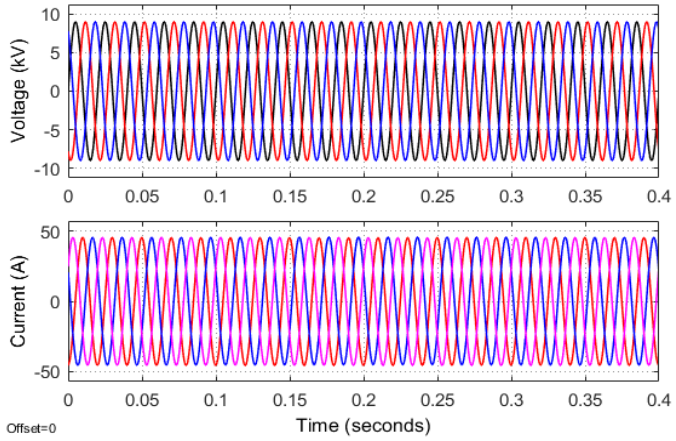


(a)

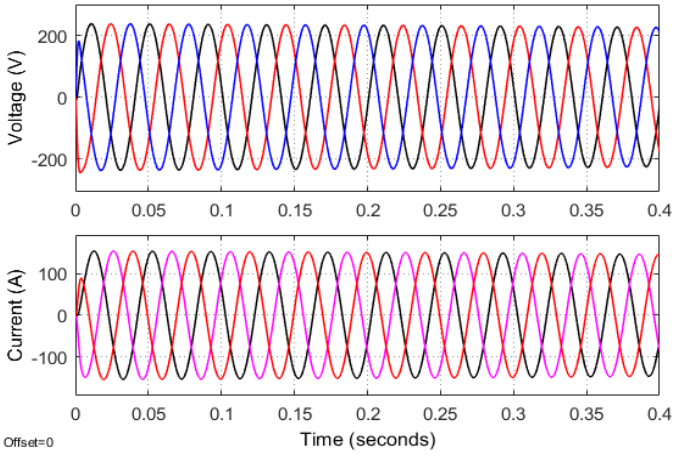


(b)

Fig. 11. Fault at line 32 (a**)** PET 1 input voltage and current, **(**b**)** PET 1 output voltage and current

### *B. Performance of PET under Load Variation*

The simulation results of an increase in the connected load at the low voltage side of PET 1 in Zone B by 60% (336KW) are shown in Fig. 12, while Fig. 13 shows the simulation results from the decrease in the loads in Zone B by 60% (84 kW). As can be seen in Fig. 13 (a) the primary side current and voltage maintained the same pattern before the occurrence of the load increase see Fig. 9 (b), while Fig. 13(b, c) shows that the output and load currents experience an increase in amplitude compared with the previous amplitude without load increase see Fig. 11 (b). Also, Fig.13 (b and c), shows that the output and the load current experience reduction in amplitude compared to figure 26 (b and c). The primary side current and voltage maintained the same pattern before the load reduction see Fig. 11 (a) and Fig. 13 (a).

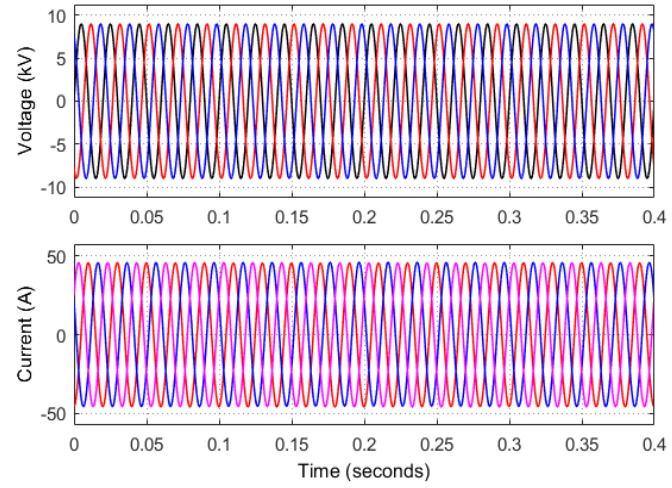


(a)

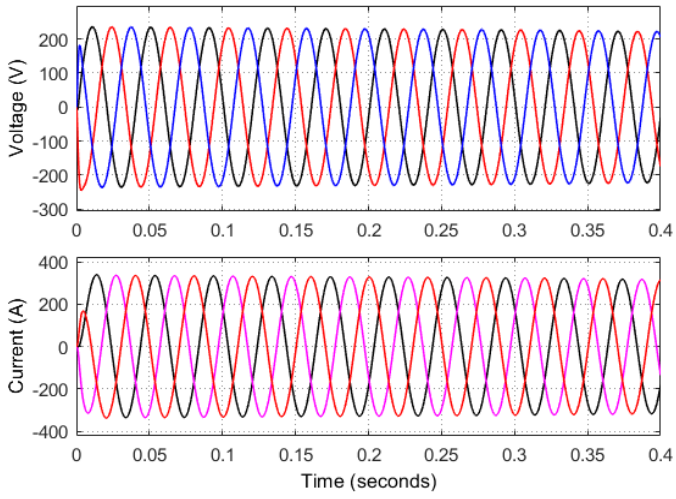


(b)

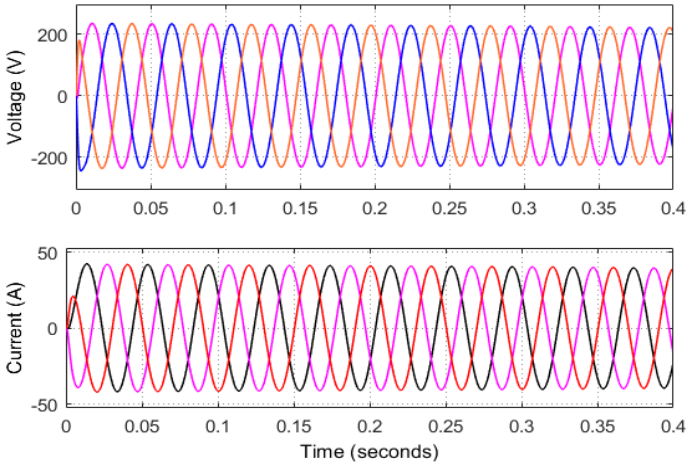


(c)

Fig. 13. Load Increase (by 60%) (a**)** PET 1 input voltage and current, **(**b**)** PET 1 output voltage and current (c**)** PET1 Load voltage and current**.**

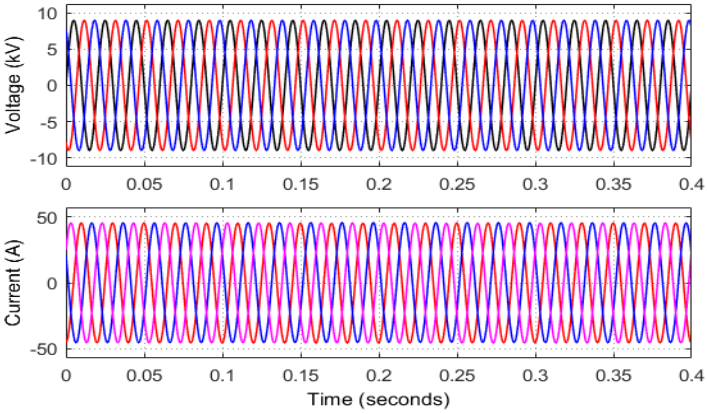


(a)

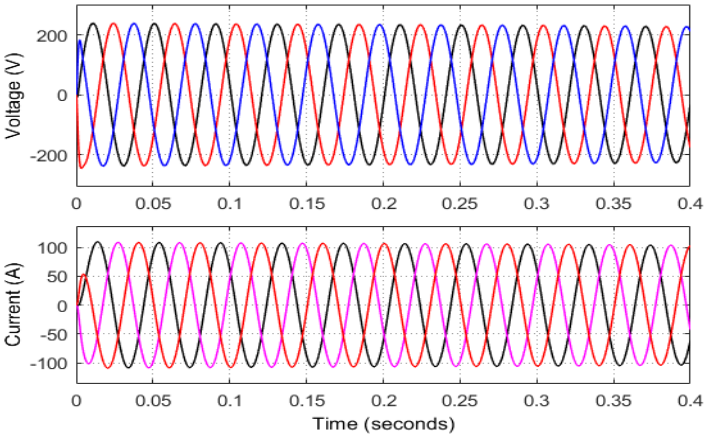


(b)

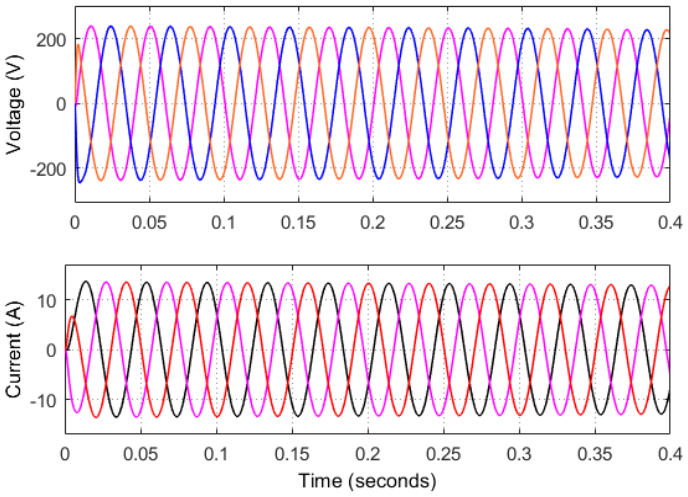


(c)

Fig. 13. Decrease load (by 60%) (a**)** PET 1 input voltage and current, **(**b**)** PET 1 output voltage and current (c**)** PET1 Load voltage and current**.**

*C. Performance of PET under voltage unbalance*

The load (LD16) connected to bus 17 at the secondary side of PET 1 in zone A was subjected to load unbalance by allocating different kW of loads to the three phases. The response of the transformer to this situation is depicted in Fig. 14. Fig. 14(b and c) shows that the secondary (output) side of the transformer experiences voltage and current phase unbalance, while the primary (Input) side voltage and current remain constant as depicted in Fig.14 (a). This shows that the load unbalances at the secondary side of the PET system did not propagate to the primary (input) side. This shows the capability of the transformer in preventing the situation across the grid with the help of the isolation stage of the transformer.

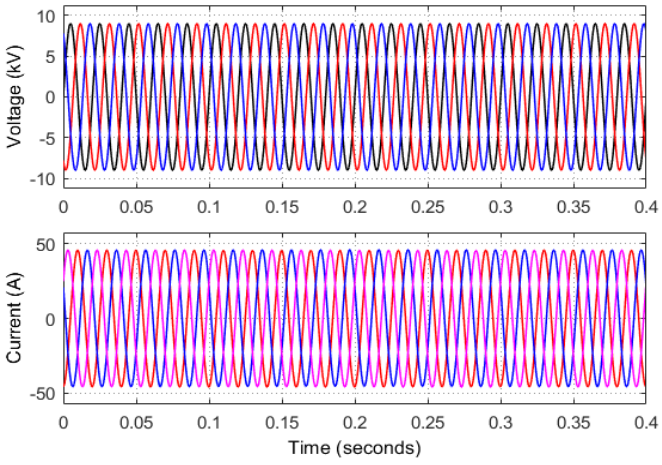


(a)

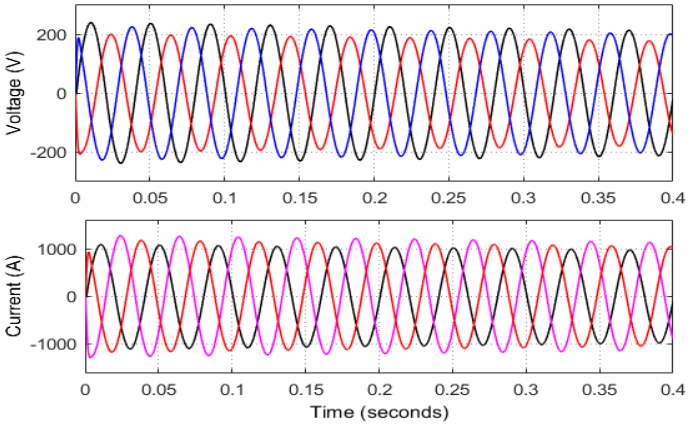


(b)

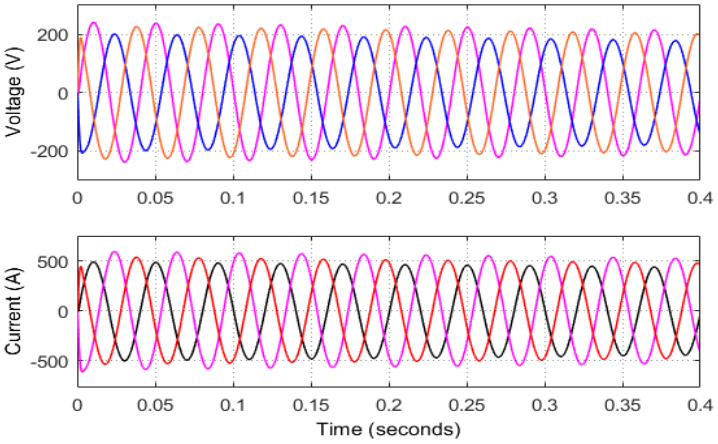


(c)

Fig. 14 Load unbalance (a) PET 1 input voltage and current, **(**b**)** PET 1 output voltage and current (c**)** PET1 Load voltage and current**.**

## IV. CONCLUSION

The design analysis and performance evaluation of an 11/0.415kV, 500 kVA unidirectional power electronic transformer in stand-alone and grid-connected modes under various power quality issues have been presented in this paper. The test system comprises 38 buses and 37 branches with 36 loads designed and simulated in Simulink. The simulation results demonstrated the capability of the PET in power quality regulation on the test system under investigation. It was observed that the Intermediate DC links provide stage decoupling and prevent perturbation from propagating from one zone of the grid to another zone. This capability was seen in the case of fault isolation and load unbalances where the voltage sag and swell were prevented by the isolation stage of the transformer from spreading from the low voltage side to medium voltage side and from medium voltage side to low voltage side of the transformer.

## APPENDIX

### Load parameters in grid connected mode

| Line | Parameters (kW) |
|---|---|
| **ZONE A** | |
| LD10 | 90 |
| LD11 | 88 |
| LD12 | 90 |
| LD13 | 90 |
| LD4 | 70 |
| **ZONE B** | |
| LD15 | 25 |
| LD16 | 25 |
| LD17 | 30 |
| LD18 | 25 |
| LD19 | 25 |
| LD20 | 30 |
| LD21 | 25 |
| LD22 | 25 |
| **ZONE C** | |
| LD31 | 50 |
| LD32 | 50 |
| LD33 | 55 |
| LD34 | 50 |
| LD35 | 58 |
| LD36 | 60 |
| LD37 | 50 |
| LD38 | 50 |
| **ZONE D** | |
| LD23 | 20 |
| LD24 | 20 |
| LD25 | 28 |
| LD26 | 20 |
| LD27 | 30 |
| LD28 | 25 |
| LD29 | 20 |

## REFERENCES

[1] A. Timbus, M. Liserre, R. Teodorescu, P. Rodriguez, and F. Blaabjerg, "Evaluation of current controllers for distributed power generation systems," IEEE Trans. Power Electron., vol. 24, no. 3, pp. 654–664, 2009.

[2] L. Byrnes, C. Brown, J. Foster, and L. D. Wagner, "Australian renewable energy policy: Barriers and challenges," Renew. Energy, vol. 60, pp. 711–721, 2013.

[3] M. N. Marwali, J. W. Jung, and A. Keyhani, "Stability analysis of load sharing control for distributed generation systems," IEEE Trans. Energy Convers., vol. 22, no. 3, pp. 737–745, 2007.

[4] M. A. Abdullah, A. P. Agalgaonkar, and K. M. Muttaqi, "Climate change mitigation with integration of renewable energy resources in the electricity grid of new south wales, Australia," Renew. Energy, vol. 66, pp. 305–313, 2014.

[5] A. Aslani and K. F. V. Wong, "Analysis of renewable energy development to power generation in the United States," Renew. Energy, vol. 63, pp. 153–161, 2014.

[6] A. Abu-Siada, J. Budiri, and A. F. Abdou, "Solid state transformers topologies, controllers, and applications: State-of-the-art literature review," Electron., vol. 7, no. 11, 2018.

[7] I. El-Samahy and E. El-Saadany, "The effect of DG on power quality in a deregulated environment," 2005 IEEE Power Eng. Soc. Gen. Meet., vol. 3, pp. 2969–2976, 2005.

[8] V. R. Pandi, H. H. Zeineldin, W. Xiao, and A. F. Zobaa, "Optimal penetration levels for inverter-based distributed generation considering harmonic limits," Electr. Power Syst. Res., vol. 97, pp. 68–75, 2013.

[9] F. Prystupczuk, V. Rigoni, A. Nouri, R. Ali, A. Keane, and T. O'Donnell, "Hybrid Power Electronic Transformer Model for System-Level Benefits Quantification in Energy Distribution Systems," Front. Electron., vol. 2, no. September, pp. 1–13, 2021.

[10] A. S. Safigianni, V. C. Poulios, and G. N. Koutroumpezis, "Penetration of mixed distributed generators in a medium voltage network," Proc. Univ. Power Eng. Conf., 2012.

[11] M. Prodanović and T. C. Green, "High-quality power generation through distributed control of a power park microgrid," IEEE Trans. Ind. Electron., vol. 53, no. 5, pp. 1471–1482, 2006.

[12] P. Pijarski, P. Kacejko, and M. Wancerz, "Voltage Control in MV Network with Distributed Generation—Possibilities of Real Quality Enhancement," Energies, vol. 15, no. 6, p. 2081, 2022.

[13] M. Kang, P. N. Enjeti, and I. J. Pitel, "Analysis and design of electronic transformers for electric power distribution system," IEEE Trans. Power Electron., vol. 14, no. 6, pp. 1133–1141, 1999.

[14] E. R. Ronan, S. D. Sudhoff, S. F. Glover, and D. L. Galloway, "A power electronic-based distribution transformer," IEEE Trans. Power Deliv., vol. 17, no. 2, pp. 537–543, 2002.

[15] D. Wang, C. Mao, J. Lu, S. Fan, and F. Peng, "Theory and application of distribution electronic power transformer," Electr. Power Syst. Res., vol. 77, no. 3–4, pp. 219–226, 2007.

[16] X. She, A. Q. Huang, and R. Burgos, "Review of solid-state transformer technologies and their application in power distribution systems," IEEE J. Emerg. Sel. Top. Power Electron., vol. 1, no. 3, pp. 186–198, 2013.

[17] J. S. Lai, "Power conditioning circuit topologies," IEEE Ind. Electron. Mag., vol. 3, no. 2, pp. 24–34, 2009.

[18] X. She, X. Yu, F. Wang, and A. Q. Huang, "Design and demonstration of a 3.6kV-120V/10KVA solid state transformer for smart grid application," Conf. Proc. - IEEE Appl. Power Electron. Conf. Expo. - APEC, pp. 3429–3436, 2014.

[19] S. Alepuz, F. González-Molina, J. Martin-Arnedo, and J. A. Martinez-Velasco, "Development and testing of a bidirectional distribution electronic power transformer model," Electr. Power Syst. Res., vol. 107, pp. 230–239, 2014.

[20] D. Wang et al., "A 10-kV/400-V 500-kVA Electronic Power Transformer," IEEE Trans. Ind. Electron., vol. 63, no. 11, pp. 6653–6663, 2016.

[21] J. Shi, W. Gou, H. Yuan, T. Zhao, and A. Q. Huang, "Research on voltage and power balance control for cascaded modular solid-state transformer," IEEE Trans. Power Electron., vol. 26, no. 4, pp. 1154–1166, 2011.

[22] X. She, "Review of SST in the Distribution System From Components to Field Application," pp. 4077–4084, 2012.

[23] S. Bird and S. Doss, "Intelligent universal transfomer desing and applications," 20 th Int. Conf. Electr. Distrib. Pap. 1032, no. 1032, pp. 8–11, 2009.

[24] L. Heinemann and G. Mauthe, "The universal power electronics based distribution transformer, an unified approach," PESC Rec. - IEEE Annu. Power Electron. Spec. Conf., vol. 2, pp. 504–509, 2001.

[25] M. E. Adabi, J. A. Martinez-Velasco, and S. Alepuz, "Modeling and simulation of a MMC-based solid-state transformer," Electr. Eng., vol. 100, no. 2, pp. 375–387, 2018.

[26] A. Dannier and R. Rizzo, "An overview of Power Electronic Transformer: Control strategies and topologies," SPEEDAM 2012 - 21st Int. Symp. Power Electron. Electr. Drives, Autom. Motion, pp. 1552–1557, 2012.

[27] D. Wang, C. Mao, and J. Lu, "Modelling of electronic power transformer and its application to power system," IET Gener. Transm. Distrib., vol. 1, no. 6, pp. 887–895, 2007.

[28] J. Tian et al., "Control of electronic power transformer with star configuration under unbalanced load conditions," Electr. Power Components Syst., vol. 42, no. 1, pp. 70–82, 2014.

[29] S. H. Hwang, X. Liu, J. M. Kim, and H. Li, "Distributed digital control of modular-based solid-state transformer using DSP+FPGA," IEEE Trans. Ind. Electron., vol. 60, no. 2, pp. 670–680, 2013.

[30] H. Wrede, V. Staudt, and A. Steimel, "Design of an electronic power transformer," IECON Proc. (Industrial Electron. Conf., vol. 2, no. 0, pp. 1380–1385, 2002.

[31] D. Wang, C. Mao, J. Lu, J. He, and H. Liu, "Auto-balancing transformer based on power electronics," Electr. Power Syst. Res., vol. 80, no. 1, pp. 28–36, 2010.

[32] H. Qin and J. W. Kimball, "Ac-Ac dual active bridge converter for solid state transformer," 2009 IEEE Energy Convers. Congr. Expo. ECCE 2009, no. c, pp. 3039–3044, 2009.

[33] K. Basu and N. Mohan, "A single-stage power electronic transformer for a three-phase PWM AC/AC drive with source-based commutation of leakage energy and common-mode voltage suppression," IEEE Trans. Ind. Electron., vol. 61, no. 11, pp. 5881–5893, 2014.

[34] B. Zhao, Q. Song, and W. Liu, "A Practical Solution of High-Frequency-Link Bidirectional Solid-State Transformer Based on Advanced Components in Hybrid Microgrid," IEEE Trans. Ind. Electron., vol. 62, no. 7, pp. 4587–4597, 2015.

[35] H. Iman-Eini, S. Farhangi, J. L. Schanen, and M. Khakbazan-Fard, "A modular power electronic transformer based on a cascaded H-bridge multilevel converter," Electr. Power Syst. Res., vol. 79, no. 12, pp. 1625–1637, 2009.

[36] J. S. Lai, A. Maitra, A. Mansoor, and F. Goodman, "Multilevel intelligent universal transformer for medium voltage applications," Conf. Rec. - IAS Annu. Meet. (IEEE Ind. Appl. Soc., vol. 3, pp. 1893–1899, 2005.

[37] T. Zhao, G. Wang, S. Bhattacharya, and A. Q. Huang, "Voltage and power balance control for a cascaded h-bridge converter-based solid-state Transformer," IEEE Trans. Power Electron., vol. 28, no. 4, pp. 1523–1532, 2013.

[38] H. Açıkgöz, Ö. F. Keçecioğlu, A. Gani, C. Yıldız, and M. Şekkeli, "Optimal Control and Analysis of Three Phase Electronic Power Transformers," Procedia - Soc. Behav. Sci., vol. 195, pp. 2412–2420, 2015.

[39] K. Y. Ahmed, N. Z. Yahaya, V. S. Asirvadam, K. Ramani, and N. M. Shannan, "Modeling of steady state and transient state of the power electronic distribution transformer," Lect. Notes Electr. Eng., vol. 398, pp. 807–817, 2017.

[40] C. Ling, B. Ge, D. Bi, and Q. Ma, "An effective power electronic transformer applied to distribution system," 2011 Int. Conf. Electr. Mach. Syst. ICEMS 2011, 2011.

[41] K. Y. Ahmed, N. Z. Yahaya, V. S. Asirvadam, and O. Ibrahim, "Modeling and Simulation of Power Electronic Distribution Transformer Based on a Three Level Converter," Appl. Mech. Mater., vol. 785, pp. 151–155, 2015.

[42] V. Blasko and V. Kaura, "A new mathematical model and control of a three-phase AC-DC voltage source converter," IEEE Trans. Power Electron., vol. 12, no. 1, pp. 116–123, 1997.

## AUTHORS

Ereola Aladesanmi, PhD, University of KwaZulu-Natal, Durban, South Africa, ereolaa@yahoo.com.
Ainah Priye Kenneth, PhD, Niger Delta University, Amassoma, Wilberforce Island Bayelsa State, ainahpriye@ndu.edu.ng

**Correspondence Author** – Ainah Priye Kenneth, ainahpriye@ndu.edu.ng.